

Weld Distortion and Residual Stresses in Aluminum Hollow Section T-Joint

Asghar Mahdian*

Faculty of Mechanics,
Malek Ashtar University of Technology, Isfahan, Iran
E-mail: A.mahdian@mut-es.ac.ir

*Corresponding author

Arash Babamiri

Faculty of Mechanics,
Malek Ashtar University of Technology, Isfahan, Iran
E-mail: arash.babamiri71@gmail.com

Behrooz Shahriari

Faculty of Mechanics,
Malek Ashtar University of Technology, Isfahan, Iran
E-mail: shahriari@mut-es.ac.ir

Received: 1 July 2021, Revised: 26 October 2021, Accepted: 10 November 2021

Abstract: Welding is known as one of the most popular attaching methods for different hollow section components. However, local concentrated heating, distortion, and residual stresses at welded joints are unavoidable. In this article, the welding simulation for rectangular hollow (RHS) sections for the front axle carrier of the new BMW series-7 is discussed and weld distortion and residual stresses in its aluminum T-joint for one proposed sequence are investigated. Comparisons of the results of this paper for this recommended sequence with experimental results in some references show good agreement and indicate that characteristics of the welding distortions are fully forecasted. In the following of this paper, the Finite Element Method (FEM) is used to offer a better sequence with smaller weld distortion and residual stresses. Weld distortion and residual stresses are highly influenced by welding strategy. In the proposed strategy, the needed time to perform the welding process decreased, and the total weld distortion and residual stresses decreased by 24% and 4%, respectively.

Keywords: Finite Element Method, Hollow Section, Residual Stresses, Welding Distortion, Weld Sequence

How to cite this paper: Asghar Mahdian, Arash Babamiri, and Behrooz Shahriari, "Weld Distortion and Residual Stresses in Aluminum Hollow Section T-Joint", Int J of Advanced Design and Manufacturing Technology, Vol. 15/No. 1, 2022, pp. 109–114. DOI: 10.30495/admt.2022.1934601.1296.

Biographical notes: **Asghar Mahdian** received his PhD in Mechanical Engineering from Isfahan University of Technology in 2011. He is currently an Assistant Professor at the Faculty of Mechanics, Malek Ashtar University of Technology, Isfahan, Iran. His current research interest includes vehicles. **Arash Babamiri** received his MSc from Mechanical Engineering at the Malek Ashtar University of Technology, Isfahan, Iran in 2016. His current research focuses on structural mechanics. **Behrooz Shahriari** received his PhD in Aerospace Engineering from Malek Ashtar University of Technology in 2016. He is currently an Assistant Professor at the Faculty of Mechanics, Malek Ashtar University of Technology.

1 INTRODUCTION

The automotive industry is developed with significant speed in the last decades and is widely used all around the world and like other important industries, “cost management” has much importance for designers. Therefore, numerical simulation can be used to reduce costs significantly. Welding and its distortion are among the inevitable parts of fabrication in the welded structure which required to attach parts and also reduce costs of assembly. To achieve the desired result, simulation of the phenomenon at an early level of the manufacture is crucial.

Weld distortion is generally governed by three factors including; material properties of base and weld metal, manufacturing process, and design specification (e.g., joint shape geometry, type of groove, and plate thickness) [1]. There are a few strategies used to control and reduce weld distortion that is well-established by Tsai et al. [2]. Weld sequence is an easy strategy to control weld distortion. Recently in the past few years, many researchers attempted to predict weld distortion and discussed the importance of weld sequences to control weld distortion. Bachorski et al. [3] used the Finite Element Method (FEM) to predict distortion during the gas metal arc welding process. To achieve this goal, they used the Shrinkage Volume Approach (SVA). Hackmair et al. [4] investigated simulation of the welding sequences and their effects on distortions in the front axle carrier of the new BMW series-7. For more complex structures, they developed a special methodology called the “Local/Global Approach”. Vural et al. [5] examined the effects of welding fixtures used to prevent distortions during the cooling process. They presented that: a) Distortions were reduced using the specially designed fixture, b) The preheating effect of the previous weld on the next weld increased distortions on the other side of the part, and c) Increase in welding speed affecting the weld heat input directly increased distortions. Fu et al. [6] studied the influence of the welding sequence on residual stresses and distortion of fillet welded structures. They employed Goldak's double ellipsoidal and optimum weld sequence to mode the heat source.

In this paper, two rectangular aluminium hollow sections were jointed together using fillet welding. A thermo-elastic FEM analysis is used to estimate weld distortion, stresses field distribution. According to welding simulation and test results of the front axle carrier of the new BMW series-7 [4] weld distortion and residual stresses in its aluminum T joint are fully reproduced. In the following of this paper, as a result of simulations, a better sequence with smaller weld distortion and residual stresses is offered. This welding sequence will reduce the distortions up to 50 percent with respect to the proposed method in the reference.

2 FEM MODEL

The Finite Element Method (FEM) is developed to calculate stress distribution and welding deformations of fillet-welded joints. Figure 1 presents the configuration and profile geometry of two rectangular hollow sections (RHS) [4]. The length of the horizontal and vertical boxes is 250 and 500 mm, respectively, and they are joined together perpendicularly. These RHSs are manufactured using aluminum alloy 6060 T6, which mechanical properties are represented in “Table 1” [7-8].

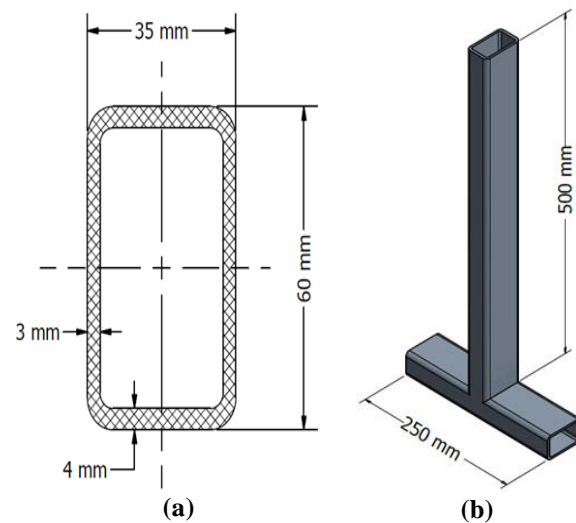


Fig. 1 (a): Dimensions of RHSs profile, and (b): configuration of RHSs in space.

Table 1 Temperature dependent properties of Aluminum 6060

Properties, 25 (°C)	
E (GPa)	70
Poisson's ratio	0.3
Yield Stress (MPa)	170
Stress (MPa) (At Strain = 1)	220
Conductivity (W/m.K)	210
Thermal Expansion	22e-6
Specific Hear Capacity (J/Kg.K)	900
Properties, 100 (°C)	
E (GPa)	65
Poisson's ratio	0.3
Yield Stress (MPa)	150
Stress (MPa) (At Strain = 1)	180
Specific Hear Capacity (J/Kg.K)	930
Properties, 200 (°C)	
E (GPa)	60
Poisson's ratio	0.3
Yield Stress (MPa)	100
Stress (MPa) (At Strain = 1)	100
Properties, 300 (°C)	
E (GPa)	45
Poisson's ratio	0.3

Yield Stress (MPa)	40
Stress (MPa) (At Strain = 1)	40
Properties, 400 (°C)	
E (GPa)	30
Poisson's ratio	0.3
Yield Stress (MPa)	20
Stress (MPa) (At Strain = 1)	20
Properties, 500 (°C)	
E (GPa)	15
Poisson's ratio	0.3
Yield Stress (MPa)	10
Stress (MPa) (At Strain = 1)	10
Specific Hear Capacity (J/Kg.K)	1100
Properties, 600 (°C)	
E (GPa)	1
Poisson's ratio	0.3
Yield Stress (MPa)	1
Stress (MPa) (At Strain = 1)	1
Conductivity (W/m.K)	260
Thermal Expansion	26e-6
Specific Hear Capacity (J/Kg.K)	1130

Two caps of the horizontal box are clamped, and the top side of the vertical box is free. Ambient temperature and convection heat transfer coefficient are 25 °C and 10 W/m²k, respectively. To attach these two boxes, four weld beads were used. Figure 2 presents the proposed strategy of welding sequence from the ref. [4].

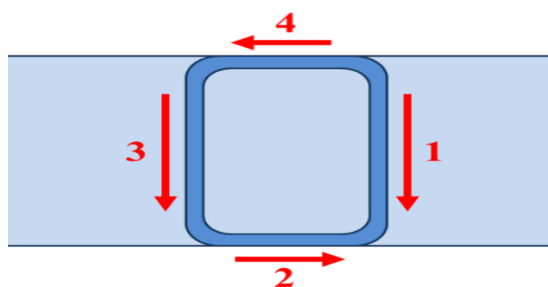


Fig. 2 Weld direction and sequence for first strategy.

The FEM numerical simulation is implemented using ABAQUS. Figure 3 presents the way model meshed. The model mesh type is 3D and the number of elements is 21421. To improve the accuracy of the calculations, Figure clearly shows that adopted mesh density near the weld area is much higher in comparison with other areas.

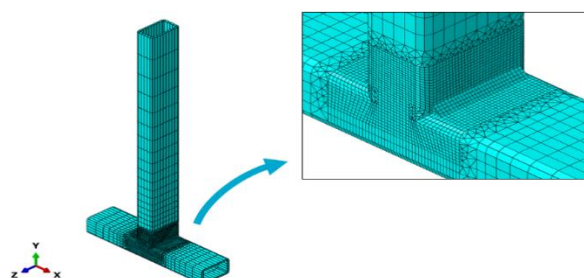


Fig. 3 Meshed model using 3D elements.

3 RESULTS

To determine the temperature field, four reference points were located on each side of the vertical tube with an equal distance of 10 mm from weld seams, titled T1-T4, respectively. Each reference point is located in the middle of the sides.

Figure 4 presents the temperature distribution contour for the first strategy (strategy-A), and “Fig. 5” shows the temperature variation changes during the welding process in terms of time (sec) for four stated reference points. Besides, “Fig. 6” presents the field contours 6, 13, 20, and 40 seconds after the end of the welding process (note that these contours show how the welded structure is cooling).

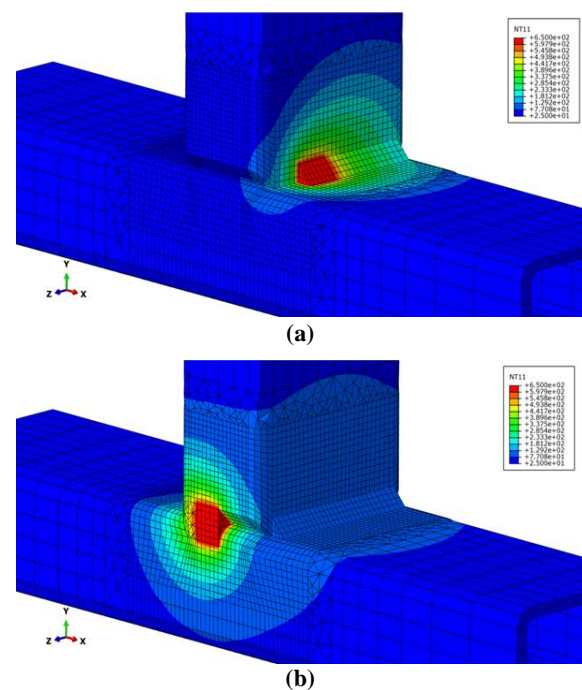


Fig. 4 (a): Temperature contour of welding at first edge, and(b): Temperature contour of welding at second edge.

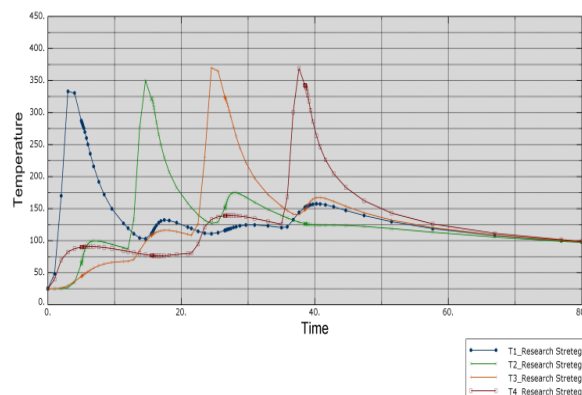


Fig. 5 Temperature variation during the welding process in term of time (sec) for stated reference points.

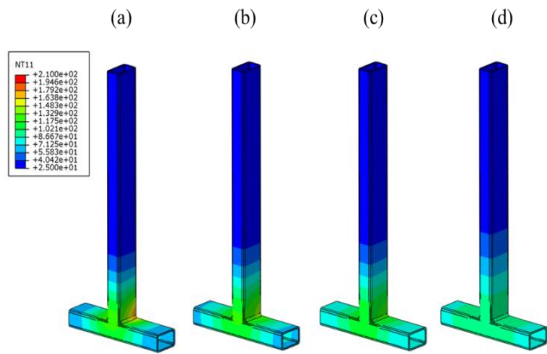


Fig. 6 Cooling process; Temperature field: (a): 6 seconds, (b): 13 seconds, (c): 20 seconds, and (d): 40 seconds after welding process.

To validate our calculated temperature field results, Ref. [4] is used. Figure 7 presents temperature variation using our FEM Strategy-A and [4] which shows good agreements between results. Here, S and M refer to the calculated and measured temperature, respectively. Our Model is similar to the model investigated in Ref. [4], but Hackmaier et al. used SYSWELD for their modeling.

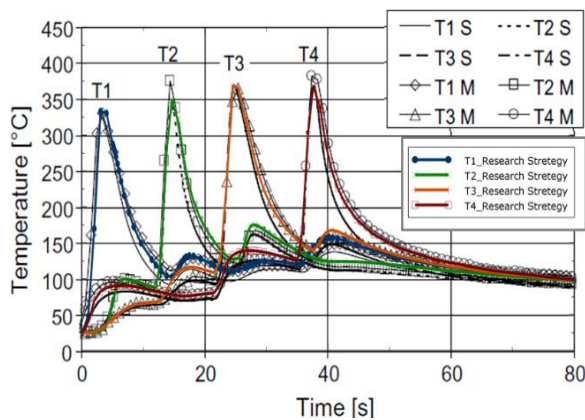


Fig. 7 Temperature variation comparison for reference points between Ref. [4] and present simulation.

As mentioned earlier, another important factor is residual stresses due to the welding process which is presented in “Fig. 8”.

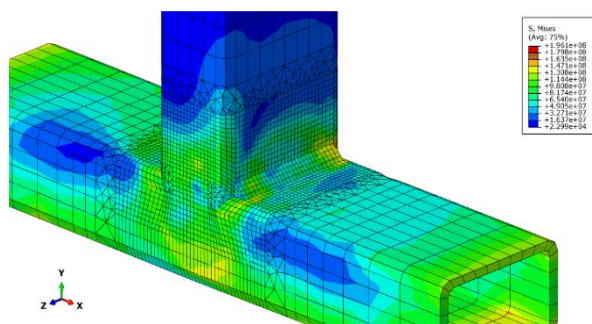


Fig. 8 Residual stresses distribution in the welded structure.

To find the best strategy for welding, displacement in the x-direction is required to be calculated. Therefore, displacement along x-direction for the top of the vertical box is simulated, and presented in “Fig. 9”.

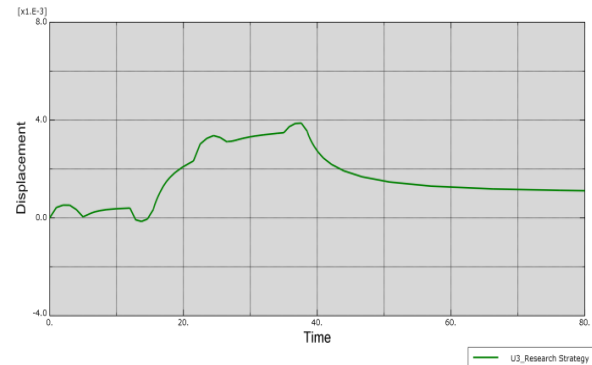


Fig. 9 Distortion variation at top of vertical tube during the welding and cooling processes.

Again, to validate the calculated distortion, results were compared with [4] which is presented in “Fig. 10”. Here again, comparison shows good agreement of the results. It should be noticed that in this figure, S refers to calculated displacement with simulation and M is an experimental measurement of displacement. Regard that using Strategy-A to perform the welding process leads to two problems; first, this procedure is hard to do for operators even for expertise; second, there is discontinuation in this welding procedure, which can cause more distortion. To overcome these defects, a new strategy is proposed (Strategy-B), simulated, and the results were compared with the previous strategy.

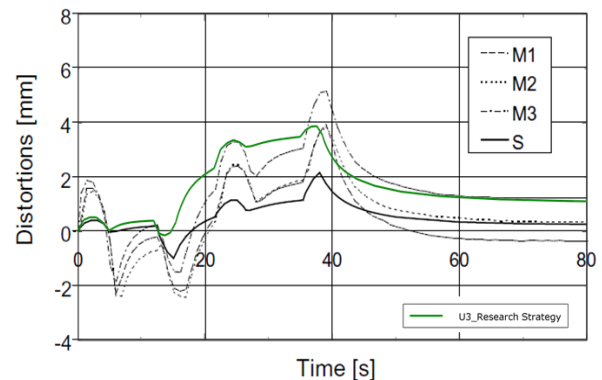


Fig. 10 Displacement comparison between experimental measurement (M), simulation calculation (S) and the present work simulation.

Figure 11 presents a new procedure for welding as the second strategy called (Strategy-B). The only difference between these two simulations is their employed welding arrangement strategy. In this new strategy, the path of welding is a continuous line that can reduce the

total time of welding, and it is more user-friendly and easier to do.

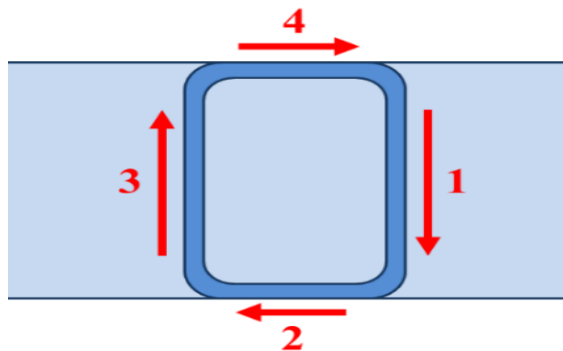


Fig. 11 New proposed strategy of welding procedure.

Figure 12 presents the time-temperature diagrams of the four specified reference points in both strategies. It should be stated that the total time of welding was reduced due to the continuity of the welding line.

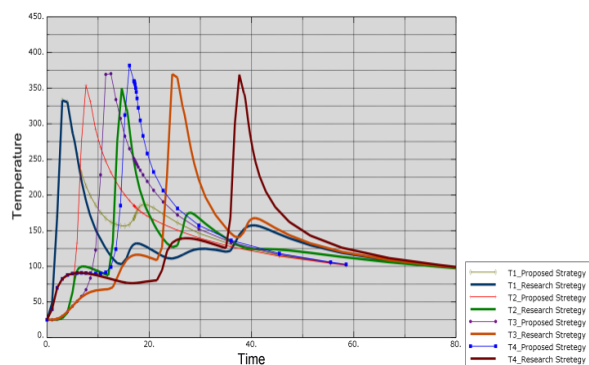


Fig. 12 Temperature variation for specified points using both strategies.

Figure 13 presents a comparison of distortion at both strategies. In this figure, U1, U3, and magnitude displacement (U) were compared. As can be seen, the proposed strategy has a lower magnitude of displacement.

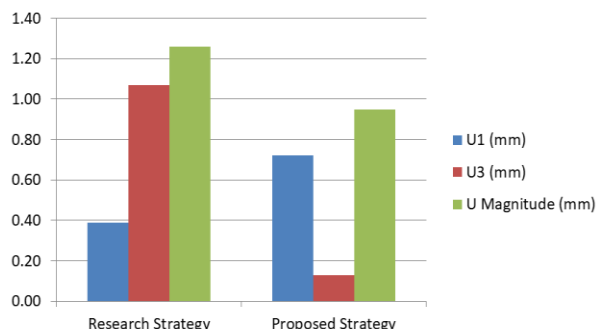


Fig. 13 Temperature variation for specified points using both strategies.

Finally, As the last part of the comparison, residual stress is simulated for both strategies. Figure 14 presents the contour of residual stress for both strategies. Maximum residual stress in the second strategy was reduced approximately 4 percent in comparison with the first strategy.

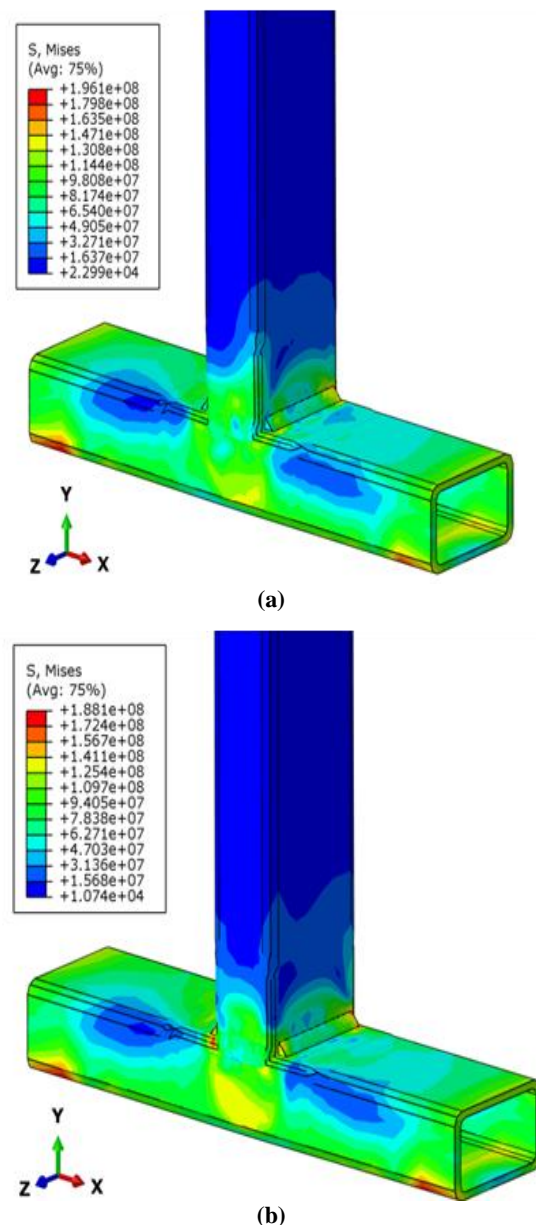


Fig. 14 Residual stresses after welding for the both strategies, (a): A(research), and (b): B(present).

4 CONCLUSIONS

In this paper, temperature field, distortion, and residual stresses caused by welding for two different strategies were investigated. model manufactured of two

aluminum alloy 6060 T6 boxes were joined perpendicularly. To have a good comparison, four reference points were located on each side of the vertical rectangular box with an equal distance of 10 mm from weld seams. Two strategies, A and B, were investigated, and the optimum strategy was specified. Simulating these two strategies represents that weld distortion, residual stresses, and temperature are highly influenced by welding strategy. In the proposed strategy (strategy-B), in comparison with case A, the total weld distortion decreased by 24% approximately, the highest temperature increased by 4% approximately, and the residual stresses decreased by 4% approximately. Also, the needed time to perform the welding process decreased using the second strategy. Considering the differences between these two strategies mentioned above using a second strategy is recommended.

REFERENCES

- [1] Murakawa, H., Deng, D., Rashe, S., and Sato, S., Prediction of Distortion Produced On Welded Structures During Assembly Using Inherent Deformation and Interface Element, Transactions of JWRI, Vol. 38, No. 2, 2009, pp. 63-69.
- [2] Tsai, C. L., Cheng, W. T., and Lee, T., Modelling Strategy for Control of Welding-Induced Distortion. Modelling of Casting, Welding and Advanced Solidification Processes VII, the Minerals, Metals and Materials Society, 1995, pp. 335-345.
- [3] Bachorski, A., Painter, M. J., Smailes, A. J., and Wahab, M. A., Finite-Element Prediction of Distortion During Gas Metal Arc Welding Using the Shrinkage Volume Approach, Journal of Materials Processing Technology, Vol. 92, 1999, pp. 405-409.
- [4] Hackmair, C., Werner, E., and Pönisch, M., Application of Welding Simulation for Chassis Components Within the Development of Manufacturing Methods, Computational Materials Science, Vol. 28, No. 3, 2003, pp. 540-547.
- [5] Vural, M., Muzafferoglu, H., and Tapici, U., The Effect of Welding Fixtures On Welding Distortions, J Achiev Mater Manuf Eng, 2007, pp. 511-514.
- [6] Guangming, F., Marcelo, I., Menglan, D., Segen, F., Influence of the Welding Sequence On Residual Stress and Distortion of Fillet Welded Structures, Marine Structures, Vol. 46, 2016, pp. 30-55.
- [7] Summers, P., Chen, Y., Rippe, Ch., Allen, B., Mouritz, A., Case, S., and Lattimer, B., Overview of Aluminum Alloy Mechanical Properties During and After Fires, in Fire Science Reviews, Vol. 4, 2015.
- [8] Incropera F., Dewitt D., Fundamentals of Heat and Mass Transfer, Wiley, New York, 1996.